DESIGN OF RECURRENT FUZZY NEURAL NETWORK AND GENERAL REGRESSION NEURAL NETWORK CONTROLLER FOR TRAVELING-WAVE ULTRASONIC MOTOR

Tien-Chi Chen[1], Tsai-Jiun Ren[2] and Yi-Wei Lou[1]

[1]Department of Electrical Engineering, Kun Shan University, Tainan, Taiwan
[2]Department of Information Engineering, Kun Shan University, Tainan, Taiwan

Keywords: Traveling-wave ultrasonic motor, TWUSM, Recurrent fuzzy neural network, RFNN, Back-propagation algorithm, Lyapunov theorem, General regression neural network, GRNN, Dead-zone.

Abstract: The traveling-wave ultrasonic motor (TWUSM) has significant features such as high holding torque at low speed range, high precision, fast dynamics, simple structure, no electromagnetic interference. The TWUSM has been used in many practical areas such as industrial, medical, robotic, and automotive applications. However, the dynamic model of the TWUSM motor has the nonlinear characteristic and dead-zone problem which varies with many driving conditions. This paper presents a novel control scheme, recurrent fuzzy neural network (RFNN) and general regression neural network (GRNN) controller, for a TWUSM control. The RFNN provides a real-time control such that the TWUSM output can track the reference command. The back-propagation algorithm is applied in the RFNN to automatically adjust the parameters on-line. The adaptive laws of the RFNN are derived by Lyapunov theorem such that the stability of the system can be absolute. The GRNN controller is appended to the RFNN controller to compensate the dead-zone of the TWUSM system using a predefined set. The experimental results are provided to demonstrate the effectiveness of the proposed controller.

1 INTRODUCTION

In recent years, the TWUSM is a new type motor, which is driven by the ultrasonic vibration force of piezoelectric elements. It has an excellent performance and many useful features (Sashida and Kenjo, 1993), such as high torque at low speed, quiet operation, light weight and compact in size, quick response, wide velocity range, high efficiency, simple structure, easy production process, no electro-magnetic interference and so on (Ueha and Tomikawa, 1993); (Uchino, 1997). Therefore, the TWUSM can be used in many regions like industrial, medical, automotive applications, aerospace science, and accurate positioning actuators (Huafeng eu al., 2005).

The TWUSM is a new type of actuator which is different to the conventional electromagnetic motors, for instance, the control technique and the operating principles. Since the TWUSM composed of piezoelectric ceramics instead of electromagnetic windings in motor structures (Uchino, 1998), the driving principles of the TWUSM are based on the ultrasonic vibration of piezoelectric elements and mechanical frictional force (Chen et al., 2008).

However, the dynamic model of the TWUSM motor is very complicated and has the nonlinear characteristic, which varies with many driving conditions. The TWUSM parameters are nonlinear and time varying due to the temperature increasing and different motor drive operating conditions, such as driving frequency, source voltage, and load torque (Sashida and Kenjo, 1993). Moreover, the control characteristics of the TWUSM are very complex to analyze and modeling accurately (Hagood and Mcfarland, 1995).

In general, the traveling-wave ultrasonic motor drive and digital control system may apply three independent control methods which are drive frequency control, supplied voltage control and phase difference control of applied voltage. In phase difference control method, the motor shows a variable dead-zone in the control input (phase difference of applied voltages) against with operating frequency. By the way, dead-zone will due to a large static friction torque appears at low speed.

Hence, it is difficult to design a perfect angle controller which can accurate control at all times. According to practical control issues, there have been reported many speed controllers based on PI (proportional plus integral) controller uses mathematical model of the motor.

Because the control algorithms of the PI controller are simple, and the controllers have the advantages such as high-stability margin and high-reliability when the controllers are tuned properly, the PI controller can use to drive the common motors. However, the PI controller can not maintain these virtues at all times. Especially, the ultrasonic motor has the nonlinear speed characteristics which vary with drive operating conditions. In order to overcome these difficulties, the dynamic controller with adjustable parameters and online learning algorithms will be suggested for the unknown or uncertain dynamics systems (Bal and Bekiroglu, 2004); (Bal and Bekiroglu, 2005).

In the past few years, there has been much research on the applications of neural networks (NNs) in order to deal with the nonlinearities and uncertainties in control systems (Alessandri et al., 2007); (Liu, 2007); (Abiyev and Kaynak, 2008). According to the structures of the NNs, the NNs can be mainly classified as feedforward NNs and recurrent NNs (RNNs) (Lin and Hsu, 2005). It is well known that feedforward NNs is capable of approximating any continuous functions closely. But the feedforward NNs are a static mapping without the aid of delays. The feedforward NNs is unable to represent a dynamic mapping. Although, the feedforward NNs presented in much research has used to deal with delay and dynamical problems. The feedforward NNs must require a large number of neurons to express dynamical responses (Ku and Lee, 1995). Furthermore, the calculations of the weights do not update quickly and the function approximation is sensitive to the training data.

On the other hand, RNNs (Juang et al., 2009) have superior capabilities compared with feedforward NNs, such as dynamics response and the information-storing ability for later use. Since the recurrent neuron has an internal feedback loop, it captures the dynamic response of a system without external feedback through long delays. Thus, the RNNs are a dynamic mapping and displays good control performance in the presence of the unknowable and time-varying model dynamics (Stavrakouds and Theochairs, 2007). As the result which is exhibited previously, the RNNs are better suited for dynamical systems than the feedforward NNs.

Furthermore, if the number of the hidden neurons is chosen too many, the computation loading is heavy so that it is not suitable for online practical applications. If the number of the hidden neurons is chosen too less, the learning performance may not be good enough to achieve the desired control performance. To solve this problem, this scheme proposed a novel controller, recurrent fuzzy neural networks (RFNN), for maintain high accuracy.

The RFNN control has a number of attractive advantages compared to the RNN control. For example, superior modeling performance due to local modeling and the fuzzy partition of the input space, linguistic description in terms of dynamic fuzzy rules, proper structure learning based on training examples, and parsimonious models with smaller parametric complexity (Lin and Chen, 2005). Thus, RFNN systems which combine the capability of fuzzy reasoning to handle uncertain information and the capability of artificial recurrent neural networks to learn processes, is used to deal with nonlinearities and uncertainties of the TWUSM.

In spite of the perfect RFNN controller has designed, there still exists a challenge for considering the TWUSM as a plant. In the proposed RFNN control schemes, the controller is effective in handling the small characteristics variations of the motor due to the updating of the connecting weights in the RFNN. However, the RFNN controller is not able to fully compensate for the dead-zone effect, and therefore the dynamic response is deteriorated (Senjyu et al., 2002). For the reason, an angle control scheme for the TWUSM with the dead-zone compensation based on RFNN is presented in this scheme. The general regression neural networks (GRNN) is adopted to determine the dead-zone compensating input and decouple the output of the RFNN. Because of the saturation reverse effect, phase difference control is not adequate for a precise angle control. Therefore the drive frequency has to be implemented in addition, which leads to a more accurate control strategy. Thus, the GRNN based on RFNN control scheme which apply both the driving frequency and phase difference constructing as the dual-mode control method was presented. The proposed controller can take the nonlinearity into account and compensate the dead-zone of TWUSM. Further, this also provides the robust performance against the parameter variations. The usefulness and validity of the proposed control scheme is examined through experimental results. The experimental results reveal that the GRNN base on the RFNN controller maintains stable and good performance on

different motion conditions. These demonstrate the reliability of the proposed control scheme and effectiveness of the MGRNN modeling control scheme in this scheme.

2 THE CONTROL SCHEME

The nonlinear dynamic system of the TWUSM is expressed as:

$$\ddot{\theta} = f(\theta) + g(\theta)u(t) + d(t) \tag{1}$$

where $f(\cdot)$ and $g(\cdot)$ are unknown functions, and assume they are bounded. $u(t)$ is the control input, $d(t)$ is the external disturbance, and θ is rotor angle displace of the TWUSM.

The proposed control scheme, illustrated as the Figure 1, is composes of two main blocks, RFNN and GRNN controller. The RFNN provides a real-time control such that the TWUSM output can track the reference command θ_r. The back-propagation algorithm is applied in the RFNN to automatically adjust the parameters on-line. The adaptive laws of the RFNN are derived by Lyapunov Theorem such that the stability of the system can be absolute. Γ, Γ_m^T, Γ_σ^T, Γ_r^T are the training parameters of adaptive update law, and η_1, η_2, η_3, η_4, η_5 are the learning rates. The GRNN controller is appended to the RFNN controller to compensate the dead-zone of the TWUSM system using a predefined set. The GRNN controller is designed to avoid the dead-zone response of the TWUSM.
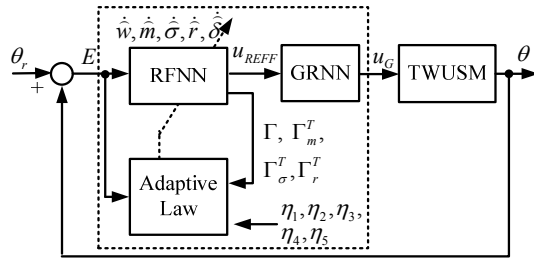

Figure 1: The control structure.

2.1 Recurrent Fuzzy Neural Networks Control System

To design a controller such that the TWUSM output can track the reference command. First, define the tracking error vector as

$$E = [e, \dot{e}]^T \tag{2}$$

where $e = \theta_r - \theta$ is the angle tracking error. From (1) and (2), an ideal controller can be chosen as

$$u^*(t) = \frac{1}{g_n(\theta)}[\ddot{\theta}_r - f_n(\theta) - d_n(t) + K^T E] \tag{3}$$

where $K = [k_2, k_1]^T$, k_1 and k_2 are positive constants. Applying (2) to (3), the error dynamics can be expressed as

$$\ddot{e} + k_1\dot{e} + k_2 e = 0 \tag{4}$$

If K is chosen to correspond to the coefficients of a Hurwitz polynomial, that is a polynomial whose roots lie strictly in the open left half of the complex plane, then the result achieved where $\lim_{t\to\infty} e(t) = 0$ for any initial conditions. Nevertheless, the functions $f(\theta)$ and $g(\theta)$ aren't accurate known and the external load disturbances is perturbed. Thus, the ideal controller $u^*(t)$ cannot be practical implemented. Therefore, the RFNN system will be designed to approximate this ideal controller.

Figure 2 shows the four-layer RFNN structure of the angle controller, which is comprised by the input layer, membership layer, rule layer, and output layer. The superscript of symbol y means the ordinal number of the layer, and the subscript of symbol y means its number. The symbol w expresses the weight of the signals. The model of RFNN is summarized as follows:

(1) **Input Layer.** The inputs of the RFNNr are $x_e^1 = e$ and $x_{\dot{e}}^1 = \dot{e}$. The outputs of input layer are $y_{e,i}^1$ and $y_{\dot{e},i}^1$, which are equal to the inputs:

$$y_{e,i}^1 = x_e^1; \quad i = 1 \sim 3 \tag{5}$$

$$y_{\dot{e},i}^1 = x_{\dot{e}}^1; \quad i = 1 \sim 3 \tag{6}$$

(2) **Membership Layer.** There are three membership functions for e, and $\dot{e}$, respectively. The three signals are sent to calculate the degree belonging to the specified fuzzy set. The outputs $y_{e,i}^2$ and $y_{\dot{e},i}^2$ are as follows.

$$y_{e,i}^2 = \exp\left(-\left(\frac{y_{e,i}^1 - m_{e,i}}{\sigma_{e,i}}\right)^2\right); \quad i = 1 \sim 3 \tag{7}$$

$$y_{\dot{e},j}^2 = \exp\left(-\left(\frac{y_{\dot{e},j}^1 - m_{\dot{e},j}}{\sigma_{\dot{e},j}}\right)^2\right); \quad i = 1 \sim 3 \tag{8}$$

where m and σ are the mean and the standard deviation of the Gaussian function. They express the

different membership functions of the RFNN, so the output of the layer can represents the belonging degree of the input to the fuzzy rule.

(3) **Rule Layer.** The outputs y_k^3 of the rule layer can be expressed as

$$y_k^3(t) = (1 + \frac{1}{1 + 100 \cdot \exp^{-10 r_k^D y_k^3(t-1)}}) y_{e,i}^2(t) y_{\dot{e},j}^2(t) \qquad (9)$$

where $k = 3 \times (i-1) + j$, $i = 1 \sim 3$, $j = 1 \sim 3$ and $k = 1 \sim 9$. r_k^D are the weights. The value of y_k^3 is always positive and between zero and two.

(4) **Output Layer.** The output y_o^4 of the RFNN can be expressed as

$$u_{RFNN} = y_o^4 = \sum_{k=1}^{9} w_k y_k^3 + \hat{\delta}\mathrm{sgn}(\mathrm{E}^T\mathrm{PB})$$
$$= w^T \Gamma(x, m, \sigma, r) + \hat{\delta}\mathrm{sgn}(\mathrm{E}^T\mathrm{PB}) \qquad (10)$$

where $\Gamma(x, m, \sigma, r) = \begin{bmatrix} y_1^3 & y_2^3 & \dots & y_9^3 \end{bmatrix}^T$ fuzzy rule function vector, and $w = \begin{bmatrix} w_1 & w_2 & \dots & w_9 \end{bmatrix}^T$ adjustable output weight vector, δ a small positive constant, and $E = \begin{bmatrix} e, \dot{e} \end{bmatrix}^T$.
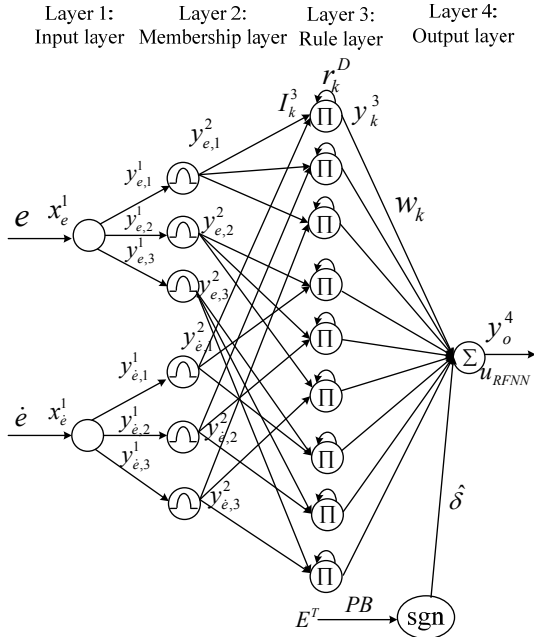

Figure 2: The structure of Recurrent Fuzzy Neural Networks.

Assume there exists an optimal RFNN to approximate the ideal control law such that

$$u^* = u^*_{RFNN}(e, w^*, m^*, \sigma^*, r^*) + \varepsilon = w^{*T}\Gamma^* + \varepsilon \qquad (11)$$

where ε is a minimum reconstructed error, w^*, m^*, σ^*, r^* and Γ^* are optimal parameters of w, m, σ, r and Γ, respectively. Thus, the RFNN control law is assumed to take the following form:

$$u = u_{RFNN} = \hat{w}^T\hat{\Gamma} + \hat{\delta}\mathrm{sgn}(\mathrm{E}^T\mathrm{PB}) \qquad (12)$$

where $\hat{w}$, $\hat{m}$, $\hat{\sigma}$, $\hat{r}$ and $\hat{\Gamma}$ are estimations of the optimal parameters, provided by tuning algorithms to be introduced later. Subtracting (12) from (11), an approximation error $\tilde{u}$ is obtained as

$$\tilde{u} = u^* - u = w^{*T}\Gamma^* + \varepsilon - \hat{w}^T\hat{\Gamma} - \hat{\delta}\mathrm{sgn}(\mathrm{E}^T\mathrm{PB})$$
$$= \tilde{w}^T\Gamma^* + \hat{w}^T\tilde{\Gamma} + \varepsilon - \hat{\delta}\mathrm{sgn}(\mathrm{E}^T\mathrm{PB}) \qquad (13)$$

where $\tilde{w} = w^* - \hat{w}$ and $\tilde{\Gamma} = \Gamma^* - \hat{\Gamma}$. The linearization technique transforms the multidimensional receptive-field basis functions into a partially linear form such that the expansion of $\tilde{\Gamma}$ in Taylor series becomes

$$\tilde{\Gamma} = \begin{bmatrix} \tilde{y}_1^3 & \dots & \tilde{y}_9^3 \end{bmatrix}^T = \Gamma_m \tilde{m} + \Gamma_\sigma \tilde{\sigma} + \Gamma_r \tilde{r} + O_v \qquad (14)$$

where $\tilde{y}_k^3 = y_k^{3*} - \hat{y}_k^3$, y_k^{3*} the optimal parameter of $\hat{y}_k^3$, $\hat{y}_k^3$ the estimated parameter of y_k^{3*}, $\tilde{m} = m^* - \hat{m}$, $\tilde{\sigma} = \sigma^* - \hat{\sigma}$, $\tilde{r} = r^* - \hat{r}$, O_v higher-order terms, $\Gamma_m = \begin{bmatrix} \partial y_1^3 / \partial m & \dots & \partial y_9^3 / \partial m \end{bmatrix}^T |_{m=\hat{m}}$, $\Gamma_\sigma = \begin{bmatrix} \partial y_1^3 / \partial \sigma & \dots & \partial y_9^3 / \partial \sigma \end{bmatrix}^T |_{\sigma=\hat{\sigma}}$ and $\Gamma_r = \begin{bmatrix} \partial y_1^3 / \partial r & \dots & \partial y_9^3 / \partial r \end{bmatrix}^T |_{r=\hat{r}}$.

Equation (14) can be rewritten as

$$\Gamma^* = \hat{\Gamma} + \Gamma_m\tilde{m} + \Gamma_\sigma\tilde{\sigma} + \Gamma_r\tilde{r} + O_v \qquad (15)$$

Substituting (15) into (13), it can be rewritten as:

$$\tilde{u} = \tilde{w}^T(\hat{\Gamma} + \Gamma_m\tilde{m} + \Gamma_\sigma\tilde{\sigma} + \Gamma_r\tilde{r} + O_v)$$
$$+ \hat{w}^T(\Gamma_m\tilde{m} + \Gamma_\sigma\tilde{\sigma} + \Gamma_r\tilde{r} + O_v) + \varepsilon - \hat{\delta}\mathrm{sgn}(\mathrm{E}^T\mathrm{PB}) \qquad (16)$$
$$= \tilde{w}^T\hat{\Gamma} + \hat{w}^T(\Gamma_m\tilde{m} + \Gamma_\sigma\tilde{\sigma} + \Gamma_r\tilde{r}) - \hat{\delta}\mathrm{sgn}(\mathrm{E}^T\mathrm{PB}) + D$$

where $D = \tilde{w}^T(\Gamma_m\tilde{m} + \Gamma_\sigma\tilde{\sigma} + \Gamma_r\tilde{r}) + w^{*T}O_v + \varepsilon$ is the uncertainty term, and this term is assumed to be bounded with a small positive constant δ (let $|D| \le \delta$). From (1), (4) and (16), an error equation is obtained

$$\dot{E} = AE + B(u^* - u) = AE + B\tilde{u}$$
$$= AE + B\begin{bmatrix} \tilde{w}^T\hat{\Gamma} + \hat{w}^T(\Gamma_m\tilde{m} + \Gamma_\sigma\tilde{\sigma} + \Gamma_r\tilde{r}) - \hat{\delta}\mathrm{sgn}(\mathrm{E}^T\mathrm{PB}) + D \end{bmatrix} \qquad (17)$$

Consider the RFNN dynamic system represented by (1), if the RFNN control law is designed as (12) with the adaptation laws for networks parameters shown in (18)–(22), the stability of the proposed RFNN control system can be guaranteed. where η_1, η_2, η_3, η_4 and η_5 are strictly positive constants.

$$\dot{\hat{w}} = \eta_1 \hat{\Gamma} E^T P B \tag{18}$$

$$\dot{\hat{m}} = \eta_2 \Gamma_m^T \hat{w} E^T P B \tag{19}$$

$$\dot{\hat{\sigma}} = \eta_3 \Gamma_\sigma^T \hat{w} E^T P B \tag{20}$$

$$\dot{\hat{r}} = \eta_4 \Gamma_r^T \hat{w} E^T P B \tag{21}$$

$$\dot{\hat{\delta}} = \eta_5 \left| E^T P B \right| \tag{22}$$

Proof:
Define a Lyapunov function candidate as

$$V(t) = \frac{1}{2} E^T P E + \frac{1}{2\eta_1} tr(\tilde{w}^T \tilde{w}) + \frac{1}{2\eta_2} \tilde{m}^T \tilde{m}$$
$$+ \frac{1}{2\eta_3} \tilde{\sigma}^T \tilde{\sigma} + \frac{1}{2\eta_4} \tilde{r}^T \tilde{r} + \frac{1}{2\eta_5} \tilde{\delta}^2 \tag{23}$$

where P is a symmetric positive definite matrix which satisfies the following Lyapunov equation

$$A^T P + P A = -Q \tag{24}$$

where Q is a positive definite matrix. Here, the estimation error of the uncertainty bound is defined as $\tilde{\delta} = \delta - \hat{\delta}$. Taking the differential of the Lyapunov function (23) and using (16) and (24), it is concluded that

$$\dot{V}(t) = -\frac{1}{2} E^T Q E + E^T P B \left[\tilde{w}^T \hat{\Gamma} + \hat{w}^T (\Gamma_m \tilde{m} + \Gamma_\sigma \tilde{\sigma} + \Gamma_r \tilde{r}) - u_C + D \right]$$
$$- \frac{1}{\eta_1} \tilde{w}^T \dot{\hat{w}} - \frac{1}{\eta_2} \tilde{m}^T \dot{\hat{m}} - \frac{1}{\eta_3} \tilde{\sigma}^T \dot{\hat{\sigma}} - \frac{1}{\eta_4} \tilde{r}^T \dot{\hat{r}} - \frac{1}{\eta_5} \tilde{\delta} \dot{\hat{\delta}} \tag{25}$$

Take (18)-(22) into (25), the derivative of V can be rewritten as

$$\dot{V}(t) = -\frac{1}{2} E^T Q E + E^T P B D - E^T P B u_C - \frac{1}{\eta_5} (\delta - \hat{\delta}) \dot{\hat{\delta}}$$
$$\leq -\frac{1}{2} E^T Q E - \left| E^T P B \right| (\delta - |D|) \leq 0 \tag{26}$$

Therefore no matter what the situation is, the derivative of V respect to time is smaller than zero. Since $\dot{V}(t) \leq 0$ is negative semi-definite (i.e., $\dot{V}(t) \leq \dot{V}(0)$), which implies E, $\tilde{w}$, $\tilde{m}$, $\tilde{\sigma}$, $\tilde{\delta}$ and $\tilde{r}$ are bounded. Let function $F(t) = E^T Q E / 2 \leq -\dot{V}(t)$, and integrate function with respect to time. Because $V(0)$ is bounded, and $V(t)$ is bounded, the following result is obtained:

$$\lim_{t \to \infty} \int_0^t F(\tau) d\tau < \infty \tag{27}$$

Also, since $\dot{F}(t)$ is bounded, so by Barbalat's Lemma, it can be shown that $\lim_{t \to \infty} F(t) = 0$. It implies that $E(t)$ will converge to zero as $t \to \infty$. As a result, the stability of the proposed control system can be guaranteed.

2.2 Convergence Analysis of RFNN

Although the stability of the adaptive RFNN control system can be guaranteed, the parameters $\hat{w}$, $\hat{m}$, $\hat{\sigma}$ and $\hat{r}$ in (18)–(21) can not be guaranteed within a bound value. The output of the RFNN is bounded, whether the means, the standard deviation of the Gaussian function and weights are bounded. Define the constrain sets $\overline{w}$, $\overline{m}$, $\overline{\sigma}$ and $\overline{r}$ respectively

$$U_w = \left\{ \|\hat{w}\| \leq \overline{w} \right\} \tag{28}$$

$$U_m = \left\{ \|\hat{m}\| \leq \overline{m} \right\} \tag{29}$$

$$U_\sigma = \left\{ \|\hat{\sigma}\| \leq \overline{\sigma} \right\} \tag{30}$$

$$U_r = \left\{ \|\hat{r}\| \leq \overline{r} \right\} \tag{31}$$

where $\| . \|$ is a two-norm of vector, $\overline{w}$, $\overline{m}$, $\overline{\sigma}$ and $\overline{r}$ are positive constants, and the adaptive laws (18)-(21) can be modified as follows

$$\dot{\hat{w}} = \begin{cases} \eta_1 \hat{\Gamma} E^T P B, & \text{if } \|\hat{w}\| < \overline{w} \text{ or } \left(\|\hat{w}\| = \overline{w} \text{ and } E^T P B \hat{w}^T \hat{\Gamma} \leq 0\right) \\ \eta_1 \hat{\Gamma} E^T P B - \eta_1 \hat{\Gamma} E^T P B \frac{\hat{w} \hat{w}^T}{\|\hat{w}\|^2}, & \text{if } \|\hat{w}\| = \overline{w} \text{ and } E^T P B \hat{w}^T \hat{\Gamma} > 0 \end{cases} \tag{32}$$

$$\dot{\hat{m}} = \begin{cases} \eta_2 \Gamma_m^T \hat{w} E^T P B, & \text{if } \|\hat{m}\| < \overline{m} \text{ or } \left(\|\hat{m}\| = \overline{m} \text{ and } E^T P B \hat{w}^T \Gamma_m \hat{m} \leq 0\right) \\ \eta_2 \Gamma_m^T \hat{w} E^T P B - \eta_2 \Gamma_m^T \hat{w} E^T P B \frac{\hat{m} \hat{m}^T}{\|\hat{m}\|^2}, & \text{if } \|\hat{m}\| = \overline{m} \text{ and } E^T P B \hat{w}^T \Gamma_m \hat{m} > 0 \end{cases} \tag{33}$$

$$\dot{\hat{\sigma}} = \begin{cases} \eta_3 \Gamma_\sigma^T \hat{w} E^T P B, & \text{if } \|\hat{\sigma}\| < \overline{\sigma} \text{ or } \left(\|\hat{\sigma}\| = \overline{\sigma} \text{ and } E^T P B \hat{w}^T \Gamma_\sigma \hat{\sigma} \leq 0\right) \\ \eta_3 \Gamma_\sigma^T \hat{w} E^T P B - \eta_3 \Gamma_\sigma^T \hat{w} E^T P B \frac{\hat{\sigma} \hat{\sigma}^T}{\|\hat{\sigma}\|^2}, & \text{if } \|\hat{\sigma}\| = \overline{\sigma} \text{ and } E^T P B \hat{w}^T \Gamma_\sigma \hat{\sigma} > 0 \end{cases} \tag{34}$$

$$\dot{\hat{r}} = \begin{cases} \eta_4 \Gamma_r^T \hat{w} E^T P B, & \text{if } \|\hat{r}\| < \overline{r} \text{ or } \left(\|\hat{r}\| = \overline{r} \text{ and } E^T P B \hat{w}^T \Gamma_r \hat{r} \leq 0\right) \\ \eta_4 \Gamma_r^T \hat{w} E^T P B - \eta_4 \Gamma_r^T \hat{w} E^T P B \frac{\hat{r} \hat{r}^T}{\|\hat{r}\|^2}, & \text{if } \|\hat{r}\| = \overline{r} \text{ and } E^T P B \hat{w}^T \Gamma_r \hat{r} > 0 \end{cases} \tag{35}$$

If the initial values $\hat{w}(0) \in U_w$, $\hat{m}(0) \in U_m$, $\hat{\sigma}(0) \in U_\sigma$ and $\hat{r}(0) \in U_r$ then the adaptive laws (32)-(35) guarantee that $\hat{w}(t) \in U_w$, $\hat{m}(t) \in U_m$, $\hat{\sigma}(t) \in U_\sigma$ and $\hat{r}(t) \in U_r$ for all $t \geq 0$.

Define a Lyapunov function as

$$v_w = \frac{1}{2} \hat{w}^T \hat{w} \tag{36}$$

And, the derivative of the Lyapunov function is presented as

$$\dot{v}_w = \hat{w}^T \dot{\hat{w}} \tag{37}$$

Assume the first line of (32) is true, either $\|\hat{w}\| < \overline{w}$ or $\left(\|\hat{w}\| = \overline{w} \text{ and } E^T P B \hat{w}^T \hat{\Gamma} \leq 0\right)$. Substituting the first line of (32) into (37), which becomes $\dot{v}_w = \eta_1 E^T P B \hat{w}^T \hat{\Gamma} \leq 0$. As a result, $\|\hat{w}\| \leq \overline{w}$ is guaranteed. In addition, when $\|\hat{w}\| = \overline{w} \text{ and } E^T P B \hat{w}^T \hat{\Gamma} > 0$,

$$\dot{v}_w = \eta_1 E^T P B \hat{w}^T \hat{\Gamma} - \eta_1 E^T P B \frac{\hat{w}^T \hat{w}}{\|\hat{w}\|^2} \hat{w}^T \hat{\Gamma} = 0 \qquad . \qquad \text{That}$$

$\|\hat{w}\| \le \bar{w}$ can be also assured. Thereby, the initial value of $\hat{w}$ is bounded, $\|\hat{w}\|$ is bounded by the constraint set $\bar{w}$ for $t \ge 0$. Similarly, it can be proved that $\|\hat{m}\|$ is bounded by the constraint set $\bar{m}$, $\|\hat{\sigma}\|$ is bounded by the constraint set $\bar{\sigma}$ and $\|\hat{r}\|$ is bounded by the constraint set $\bar{r}$ for $t \ge 0$.

When the condition $\|\hat{w}\| < \bar{w}$ or $\left(\|\hat{w}\| = \bar{w} \text{ and } E^T P B \hat{w}^T \hat{\Gamma} \le 0 \right)$, $\|\hat{m}\| < \bar{m}$ or $\left(\|\hat{m}\| = \bar{m} \text{ and } E^T P B \hat{w}^T \Gamma_m \hat{m} \le 0 \right)$, $\|\hat{\sigma}\| < \bar{\sigma}$ or $\left(\|\hat{\sigma}\| = \bar{\sigma} \text{ and } E^T P B \hat{w}^T \Gamma_\sigma \hat{\sigma} \le 0 \right)$, $\|\hat{r}\| < \bar{r}$ or $\left(\|\hat{r}\| = \bar{r} \text{ and } E^T P B \hat{w}^T \Gamma_r \hat{r} \le 0 \right)$, the stability analysis the same as (33), (34) and (35). In the other situation, the condition $\|\hat{w}\| = \bar{w}$ and $E^T P B \hat{w}^T \hat{\Gamma} > 0$, $\|\hat{m}\| = \bar{m}$ and $E^T P B \hat{w}^T \Gamma_m \hat{m} > 0$, $\|\hat{\sigma}\| = \bar{\sigma}$ and $E^T P B \hat{w}^T \Gamma_\sigma \hat{\sigma} > 0$, $\|\hat{r}\| = \bar{r}$ and $E^T P B \hat{w}^T \Gamma_r \hat{r} > 0$ is occurred, the Lyapunov function can be rewritten as follows

$$
\begin{aligned}
\dot{v}_w &= -\frac{1}{2} E^T Q E + E^T P B \left(\tilde{w}^T \hat{\Gamma} + \hat{w}^T \Gamma_m \tilde{m} + \hat{w}^T \Gamma_\sigma \tilde{\sigma} + \hat{w}^T \Gamma_r \tilde{r} \right) + D - u_C) - \frac{1}{\eta_1} \tilde{w}^T \dot{\hat{w}} \\
&\quad - \frac{1}{\eta_2} \dot{\hat{m}}^T \tilde{m} - \frac{1}{\eta_3} \dot{\hat{\sigma}}^T \tilde{\sigma} - \frac{1}{\eta_4} \dot{\hat{r}}^T \tilde{r} - \frac{1}{\eta_5} \tilde{\delta} \dot{\hat{\delta}} \\
&= -\frac{1}{2} E^T Q E + E^T P B (D - u_C) + E^T P B \frac{\tilde{w}^T \hat{w}}{\|\hat{w}\|^2} \hat{w}^T \hat{\Gamma} + (\Gamma_m^T \hat{w})^T E^T P B \hat{m} \frac{\hat{m}^T \tilde{m}}{\|\hat{m}\|^2} \\
&\quad + (\Gamma_\sigma^T \hat{w})^T E^T P B \hat{\sigma} \frac{\hat{\sigma}^T \tilde{\sigma}}{\|\hat{\sigma}\|^2} + (\Gamma_r^T \hat{w})^T E^T P B \hat{r} \frac{\hat{r}^T \tilde{r}}{\|\hat{r}\|^2} - \frac{1}{\eta_5} \tilde{\delta} \dot{\hat{\delta}}
\end{aligned}
\tag{38}
$$

Equation $\tilde{w}^T \hat{w} = \left(\|w^*\|^2 - \|\hat{w}\|^2 - \|\tilde{w}\|^2 \right) / 2 < 0$, which is according to $\|\hat{w}\| = \bar{w} > \|\hat{w}^*\|$. Similarly, $\|\hat{m}\| = \bar{m} > \|\hat{m}^*\|$, $\|\hat{\sigma}\| = \bar{\sigma} > \|\hat{\sigma}^*\|$ and $\|\hat{r}\| = \bar{r} > \|\hat{r}^*\|$ can be proved. Finally, it is obtained as

$$
\begin{aligned}
\dot{v}_w &= -\frac{1}{2} E^T Q E + E^T P B D - E^T P B u_C + E^T P B \frac{\tilde{w}^T \hat{w}}{\|\hat{w}\|^2} \hat{w}^T \hat{\Gamma} + \Gamma_m^T \hat{w} E^T P B \hat{m} \frac{\hat{m}^T \tilde{m}}{\|\hat{m}\|^2} \\
&\quad + \Gamma_\sigma^T \hat{w} E^T P B \hat{\sigma} \frac{\hat{\sigma}^T \tilde{\sigma}}{\|\hat{\sigma}\|^2} + \Gamma_r^T \hat{w} E^T P B \hat{r} \frac{\hat{r}^T \tilde{r}}{\|\hat{r}\|^2} - \frac{1}{\eta_5} \tilde{\delta} \dot{\hat{\delta}} \\
&\le -\frac{1}{2} E^T Q E + E^T P B \frac{\left(\|w^*\|^2 - \|\hat{w}\|^2 - \|\tilde{w}\|^2 \right)}{\|\hat{w}\|^2} \hat{w}^T \hat{\Gamma} \\
&\quad + \frac{1}{2} (\Gamma_m^T \hat{w})^T E^T P B \hat{m} \frac{\left(\|m^*\|^2 - \|\hat{m}\|^2 - \|\tilde{m}\|^2 \right)}{\|\hat{m}\|^2} \\
&\quad + \frac{1}{2} (\Gamma_\sigma^T \hat{w})^T E^T P B \hat{\sigma} \frac{\left(\|\sigma^*\|^2 - \|\hat{\sigma}\|^2 - \|\tilde{\sigma}\|^2 \right)}{\|\hat{\sigma}\|^2} \\
&\quad + \frac{1}{2} (\Gamma_r^T \hat{w})^T E^T P B \hat{r} \frac{\left(\|r^*\|^2 - \|\hat{r}\|^2 - \|\tilde{r}\|^2 \right)}{\|\hat{r}\|^2} \\
&\le -\frac{1}{2} E^T Q E \le 0
\end{aligned}
\tag{39}
$$

Using the same discussion shown in previous section, the stability property can be also guaranteed since $E \to 0$ as $t \to 0$.

2.3 General Regression Neural Networks Control System Design

As a common nonlinear problem, dead-zone often appears in the control system, which not only makes steady-sate error, but also deteriorates the dynamic quality of the control systems. As for the dead-zone compensation problems, general regression neural networks (GRNN) control methods is proposed to solve this problems. The GRNN is a powerful regression tool with a dynamic network structure and training speed is extremely fast. Due to the simplicity of the network structure and ease of implementation, it can be widely applied to a variety of fields.

The GRNN scheme which shows in Figure 3 is suggested for the nonlinear compensation of the system input. Where the input u is the output of the RFNN, W_G^1 is the weight of the hidden layer, W_G^2 is the weight of the output layer, a is the output of the hidden layer, u_G is the output of the output layer.
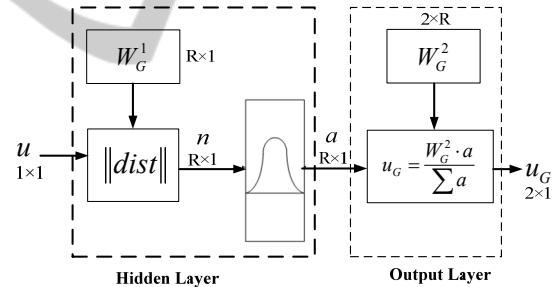

Figure 3: The structure of the GRNN.

The GRNN is composed of two layers, which are the hidden layer and the output layer. The input u of the GRNN means a torque which calculated by the RFNN. The outcome n of $\|dist\|$ is represented the Euclidean distance between input u and each elements of W_G^1. Then n pass by a Gaussian function. When the Euclidean distance between u and W_G^1 is far, the element of the output a is approach to zero. In the other hand, the Euclidean distance is short and the element of the output a is approach to one. The Gaussian function is

$$a = \exp\left(-\left(\frac{n - m}{\sigma} \right)^2 \right) \tag{40}$$

Where m and σ are the center and the stand deviation of the Gaussian function respectively. In order to increase the discrimination and have a better performance, the stand deviation σ value of the Gaussian function is chose low.

The relation function of output layer can be expressed as

$$u_G = \frac{W_G^2 \cdot a}{\sum a} \tag{41}$$

The output vector of hidden layer a is multiplied with appropriate weights W_G^2 to sum up for produce the output u_G of the GRNN. The output u_G composed of frequency control u_f and phase control u_P is expressed as

$$u_G = \begin{bmatrix} u_f & u_p \end{bmatrix}^T \tag{42}$$

Applying the GRNN controller, the dead-zone of the TWUSM will be compensated as desired.

3 EXPERIMENTS

To prove the feasibility of the scheme, the experiments are required. The structure of the experiment includes DSP program and hardware driving circuit. It is shown in the Figure 4. The TMS320F2812 DSP experiment board is applied as the computing core. The DSP program was coded by C language. After compile, assemble and link, the executing file will be generated by c2000 code composer (CCS), additionally the executing file was be executed in the same windows interface.
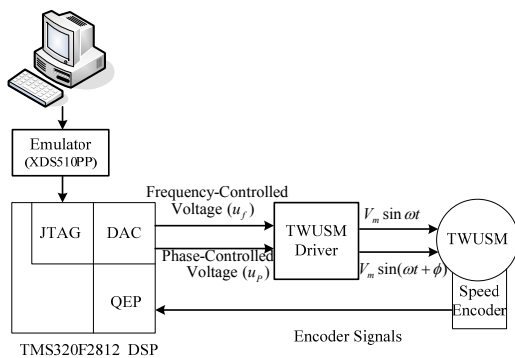

Figure 4: Experimental system of the TWUSM.

In the experiments, there are three different controllers chosen for comparison.
(i) The proposed control scheme, RFNN and GRNN controller.

(ii) The RFNN only, without GRNN controller. The control algorithm of RFNN only is the same as RFNN of the proposed control scheme.

(iii) The PI controller. The PI controller is the one of the most used controller in linear system. The control PI controller has important advantages such as simple structure and easy to design. Therefore, PI controllers are used widely in industrial application. Owing to the absence of the mathematical model of the TWUSM, the PI controller parameters are chosen by trial and error in such a way that the optimal the performance occurs at rated conditions. The block diagram of the angle control system for ultrasonic motor by PI controller shown in Figure 5. Where θ_r and θ are command and rotor angle, $e(k)$ is the tracking error, u_f is the frequency command, u_p is the phase different command, respectively. The parameters of the PI controller are selected as $K_P = 1000$ and $K_I = 100$. The parameters of the PI controller 2 are selected as $K_P = 1000$ and $K_I = 100$.
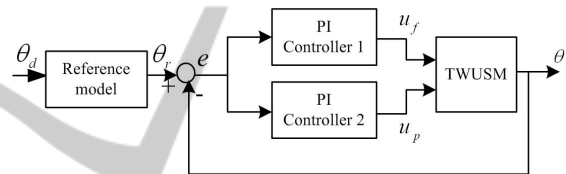

Figure 5: The block diagram of the dual-mode PI control.

Figures 6 to 8 show the experimental results of the proposed control scheme, the RFNN only, and the PI control respectively, for a periodic square angle command from -90 to 90 degree. Figures 9 to 11 show the experimental results of the proposed control scheme, the RFNN only, and the PI control respectively, for a sinusoidal angle command from -90 to 90 degree. In each Figure (a) shows the TWUSM angle response and speed response. In each Figure (b) shows the angle error between angle command and angle response.

Observing the experimental results of the proposed control scheme in Figures 6 and 9, the tracking errors both can converge to an acceptable region and the control performance is excellent. The proposed controller retains control performance and has not any dead-zone in the constructed.

The experimental results of the RFNN only in Figures 7 and 10 show that the tracking error is similar to the proposed control scheme. However, the drawbacks of the RFNN controller are interfered with the dead-zone and the motor speed has the serious chattering phenomenon in slow speed nearby zero.
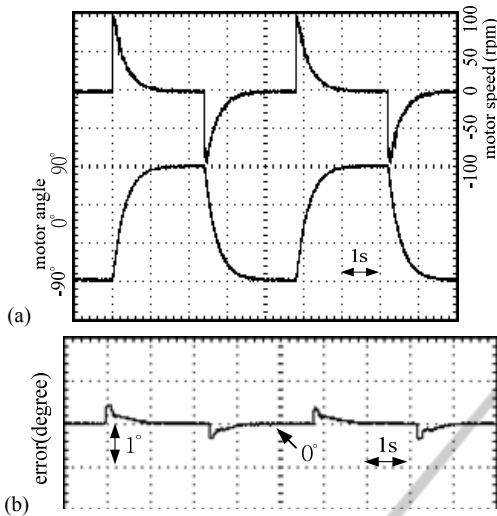
(a)

(b)

Figure 6: The experimental result of the proposed control scheme for a periodic angle square command from -90 to 90 degree.
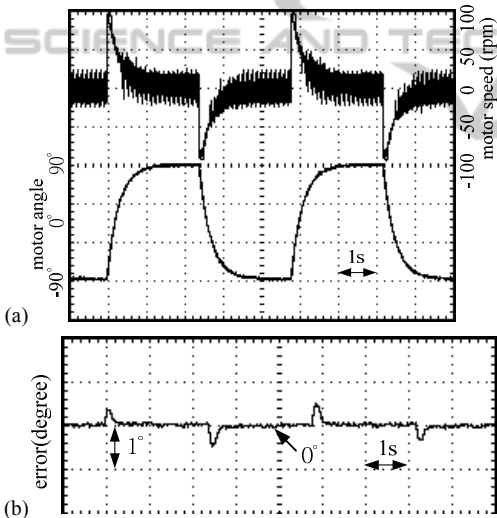

(a)

(b)

Figure 7: The experimental result of the RFNN only for a periodic square angle command from -90 to 90 degree.

In Figures 8 and 11 illustrated that the PI controller has a chattering phenomenon like the RFNN only and larger tracking error.

4 CONCLUSIONS

The proposed control scheme, RFNN and GRNN controller, has been applied to the TWUSM in the paper. Many concepts such as controller design and the stability analysis of the controller are introduced. Furthermore, experiment results are shown and proven that the proposed control scheme is feasible

and the performance of the proposed method is better than the others.
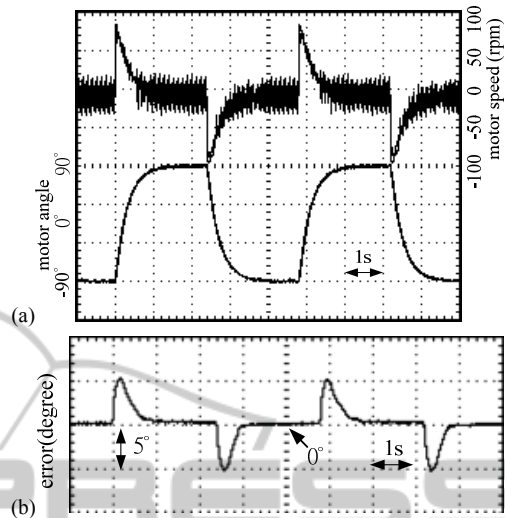

(a)

(b)

Figure 8: The experimental result of the PI control for a periodic square angle command from -90 to 90 degree.
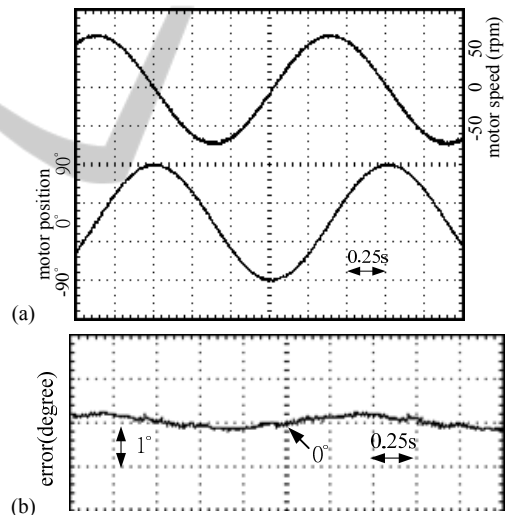

(a)

(b)

Figure 9: The experimental result of the proposed control scheme for a sinusoidal angle command from -90 to 90 degree.

The proposed control scheme includes the RFNN controller and the GRNN controller. The RFNN controller is designed to track the reference angle. The variables of membership function and weights can be updated by the adaptive algorithms. Moreover, all parameters of the proposed RFNN controller are tuned in the Lyapunov sense; thus, the stability of the system can be guaranteed. In the RFNN, a compensated controller is designed to recover the residual part of approximation error. The GRNN controller is appended to the RFNN

controller to compensate the dead-zone of the TWUSM system using a predefined set. The GRNN controller can successfully avoid the dead-zone problem of the TWUSM. The proposed controller has been verified that it can control the system well according to the experimental results.
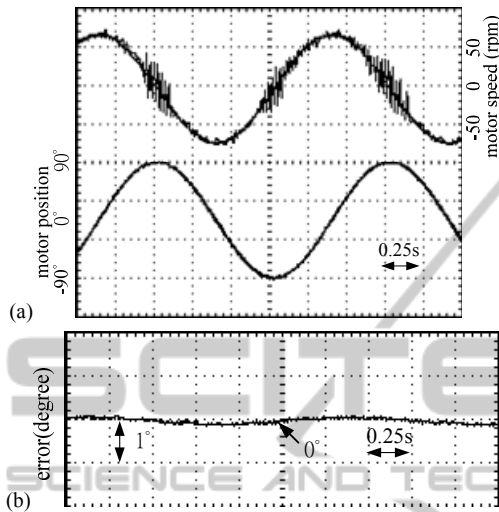

Figure 10: The experimental result of the RFNN only for a sinusoidal angle command from -90 to 90 degree.
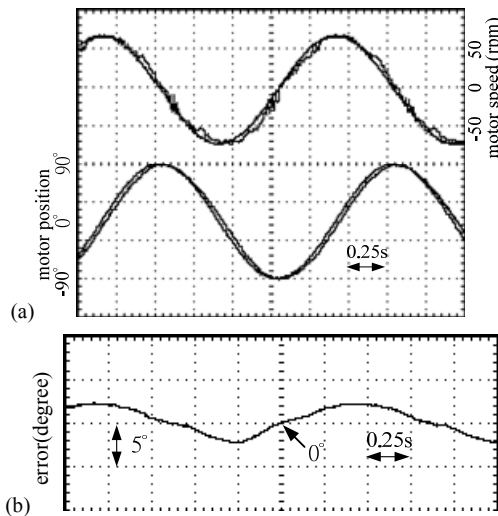

Figure 11: The experimental result of the PI control for a sinusoidal angle command from -90 to 90 degree.

ACKNOWLEDGEMENTS

REFERENCES

Sashida, T., Kenjo, T., 1993. An introduction to ultrasonic motors, *Clarendon Press*, Oxford,

Ueha, S., Tomikawa, Y., 1993. Ultrasonic motors theory and applications, *Clarendon Press*, Oxford.

Uchino, K., 1997. Piezoelectric actuators and ultrasonic motors, *Kluwer Academic Publishers*.

Huafeng, L., Chunsheng, Z., Chenglin, G., 2005. Precise position control of ultrasonic motor using fuzzy control with dead-zone compensation. *J. of Electrical Engineering, vol. 56, no. 1-2, pp. 49-52*.

Uchino, K., 1998. Piezoelectric ultrasonic motors: overview. *Smart Materials and Structures, vol. 7, pp. 273-285*.

Chen, T. C., Yu, C. H., Tsai, M. C., 2008. A novel driver with adjustable frequency and phase for traveling-wave type ultrasonic motor. *Journal of the Chinese Institute of Engineers, vol. 31, no. 4, pp. 709-713*.

Hagood, N. W., Mcfarland, A. J., 1995. Modeling of a piezoelectric rotary ultrasonic motor. *IEEE Trans. on Ultrasonics, Ferroelectrics, and Frequency control, vol. 42, no. 2, pp. 210-224*.

Bal, G., Bekiroglu, E., 2004. Servo speed control of traveling-wave ultrasonic motor using digital signal processor. *Sensor and Actuators A 109, pp. 212-219*.

Bal, G., Bekiroglu, E., 2005. A highly effective load adaptive servo drive system for speed control of traveling-wave ultrasonic motor. *IEEE Trans. on Power Electronics, vol. 20, no. 5, pp. 1143-1149*.

Alessandri, A., Cervellera, C., Sanguineti, M., 2007. Design of asymptotic estimators: an approach based on neural networks and nonlinear programming. *IEEE Trans. on Neural Networks, vol. 18, no. 1, pp. 86-96*.

Liu, M., 2007. Delayed standard neural network models for control systems. *IEEE Trans. on Neural Networks, vol. 18, no. 5, pp. 1376-1391*.

Abiyev, R. H., Kaynak, O., 2008. Fuzzy Wavelet Neural Networks for Identification and Control of Dynamic Plants-A Novel Structure and a Comparative Study. *IEEE Trans. on Industrial Electronics, vol. 55, no.8, pp. 3133-3140*.

Lin, C. M., Hsu, C. F., 2005. Recurrent neural network based adaptive -backstepping control for induction servomotors. *IEEE Trans. on Industrial Electronics, vol. 52, no. 6, pp. 1677-1684*.

Ku C. C., Lee, K. Y., 1995. Diagonal recurrent neural networks for dynamic systems control. *IEEE Trans. on Neural Networks, vol. 6, no. 1, pp. 144-156*.

Juang, C. F., Huang, R. B., Lin, Y. Y., 2009. A Recurrent Self-Evolving Interval Type-2 Fuzzy Neural Network for Dynamic System Processing. *IEEE Trans. on Fuzzy Systems, vol. 17, no. 5, pp. 1092-1105*.

Stavrakouds, D. G., Theochairs, J. B., 2007. Pipelined Recurrent Fuzzy Neural Networks for Nonlinear Adaptive Speech Prediction. *IEEE Trans. on Systems, Man and Cybernetics, Part B, vol. 37, no. 5, pp. 1305-1320*.

Lin, C. J., Chen, C. H., 2005. Identification and prediction using recurrent compensatory neuro-fuzzy systems. *Fuzzy Sets and Systems, vol. 150, no. 2, pp. 307-330.*

Senjyu, T., Kashiwagi, T., Uezato, K., 2002. Position control of ultrasonic motors using MRAC with deadzone compensation. *IEEE Trans. on Power Electronics, vol. 17, no. 2, pp. 265-272.*